

# Kinetic coefficients near the metal-insulator transition

R. O. Zaitsev

Zh. Eksp. Teor. Fiz. 85, 272–286 (July 1983)

The dc conductivity and diffusion coefficient near the metal-insulator phase-transition point (the Mott or  $M$  transition) are calculated for the low-temperature case. It is shown that the diffusion coefficient  $D$  and conductivity  $\sigma$  in the self-consistent-field approximation are proportional to the first and second powers, respectively, of the metallic order parameter  $\tilde{\omega}$ . In the region of strong correlations the fall-off of the kinetic coefficients is governed by two critical exponents. One of these,  $\beta$ , governs the fall-off of the order parameter  $\tilde{\omega}$  and the electronic density of states  $\nu: \nu \propto \tilde{\omega} \propto |\tau|^\beta$ , where  $\tau$  measures the distance from the transition point. The other exponent,  $\lambda$ , is of kinetic origin:  $D \propto \tilde{\omega} |\tau|^\lambda$ ,  $\sigma \propto \tilde{\omega}^2 |\tau|^\lambda$ . The universal critical exponents  $\beta$  and  $\lambda$  are evaluated by the renormalization-group method in the space of  $4 - \varepsilon$  dimensions.

PACS numbers: 71.30. + h, 72.10.Bg, 64.60.Fr, 66.30.Dn

## INTRODUCTION

The concept of a metallic order parameter, which was discovered by Wegner,<sup>1</sup> found immediate use in the theory of localization for systems with dimensionality  $d$  close to 2. Near the metal-insulator transition ( $M$ -transition) point all the physical singularities are determined by the law governing the vanishing of the metallic order parameter  $\tilde{\omega}$  and by fluctuations in this quantity. It has been proven<sup>2</sup> that near the  $M$ -transition point such quantities as the density of states at the Fermi level ( $\nu$ ) and the inverse square of the electrostatic screening radius ( $\kappa^2$ ) are proportional to  $\tilde{\omega}$ . In the self-consistent-field theory for  $T = 0$  these quantities go to zero as  $|\tau|^{1/2}$ , where  $\tau$  is the distance from the transition point in terms of the pressure or of the concentration of an impurity component. The role of the external magnetic field is played by the Matsubara frequency  $\omega = (2n + 1)\pi T$ , and in the region of applicability of the self-consistent-field method  $\tilde{\omega}$  obeys an equation of the Landau-Ginzburg type. In a previous paper<sup>3</sup> the present author attempted to determine the thermodynamic critical exponents for three-dimensional objects in the region of strong correlations with the aid of an  $\varepsilon$  expansion ( $\varepsilon = 4 - d$ ). It was established that the main difference between the  $M$  transition and a second-order transition lies in that for the  $M$  transition the critical exponents turn out to be different on opposite sides of the transition point. In the region of strong correlations the governing role on the insulator side of the transition ( $\tau > 0$ ) is played by localized states, which provide a "tail" on the electron energy distribution. On the side of the metallic phase the corresponding states take on a quasi-local character, and their role therefore becomes unimportant against the background of critical fluctuations. This circumstance makes it possible not only to evaluate all the thermodynamic critical exponents for the metallic phase, but also to determine the law describing the vanishing of the conductivity  $\sigma$  and diffusion coefficient  $D$ , which are related to each other and to the density of states at the Fermi level by the famous Einstein relation

$$\sigma = e^2 \nu D. \quad (1)$$

In the "tail" region of the insulator part of the phase diagram the dc conductivity is evidently of a percolational character

(or is absent altogether). All the physical phenomena are governed by the inhomogeneous distribution of the complex order parameter  $i\tilde{\omega}$ —the inhomogeneous regime in the Mott classification.<sup>4</sup> As in Ref. 3, we shall restrict discussion to the case of a half-filled band. The applicable models in this case are the Hubbard model,<sup>5</sup> the model of a nonideal excitonic insulator,<sup>6</sup> and also the symmetric model of a binary solid solution.<sup>7</sup>

In the present paper a method is devised to evaluate the kinetic coefficients in the static limit on the metal side of the transition ( $\tau < 0$ ), where, according to the assumption of Ref. 3, one can neglect the quasi-local states of the instanton type. Near the  $M$ -transition point, where  $|\tau| \ll 1$ , the energy and damping of the excitations are of the same order of magnitude.<sup>3</sup> It follows that in this region the mean free path  $l$  is of the order of the mean distance  $a$  between electrons, so that all the kinetic phenomena are governed by the diffusion regime,<sup>4</sup> where the resistivity grows from  $3 \cdot 10^{-4}$  to  $3 \cdot 10^{-3}$   $\Omega \cdot \text{cm}$ . In the first part of this paper it is shown that in this region the conductivity is proportional to  $\tilde{\omega}^2$  or to the square of the density of states, in agreement with the familiar Kubo-Greenwood formula.

In the immediate vicinity of the  $M$  transition the conductivity becomes less than  $\sigma \approx 800/a$  ( $\Omega \cdot \text{\AA}$ )<sup>-1</sup>, which was long assumed to be the minimum value of the electronic conductivity. It is in this region that one must take correlation effects into account not only for the order parameter  $\tilde{\omega}$ , but also in evaluating the transition probability, which is expressed in terms of the two-particle Green function.

In the second part of this paper it is shown that near the  $M$  transition on the metal side of the corresponding two-particle correlator admits an expansion in powers of the metallic order parameter. The coefficients of this expansion can be calculated by the renormalization-group method in the space of  $4 - \varepsilon$  dimensions. In the model of a nonideal excitonic insulator the region of strong correlation effects is extremely narrow on account of the small Ginzburg number—the ratio of the interelectron distance  $a$  to the correlation length (see Ref. 3 and below). For this reason the kinetic coefficients can be evaluated in the diffusion regime by the self-consistent-field method, which in this case has a wide

region of applicability. In the Hubbard model and in the model of a binary solid solution, the Ginzburg parameter is of the order of unity. For this reason there is no region in which the self-consistent-field method applies, and correlation effects are manifested even in the diffusion regime. It was shown in Ref. 3 that all three of the models studied have the same critical exponents, but the renormalization-group equations admit two types of solutions, which correspond to two sets of critical exponents. One solution borders on perturbation theory, but is unstable against fluctuations which are noninvariant to a time reversal—the so-called “+” model. The other solution is stable, but does not link up with perturbation theory—the so-called “-” model.

The critical exponents of the “-” model leads to weaker thermodynamic singularities than does the “+” model. For example, the character of the phase transition at  $T = 0$  is governed by the critical exponent  $\varepsilon'$ :  $\Delta E \propto |\tau|^{\varepsilon'}$ , where

$$\varepsilon' = 1 + 3\beta + \gamma = \begin{cases} 7/2 - \varepsilon/3, & \text{“+” model} \\ 7/2 + \varepsilon/2, & \text{“-” model} \end{cases} \quad (2)$$

In the approximation linear in  $\varepsilon$  one has

$$\beta = \begin{cases} 1/2 - \varepsilon/6, & \text{“+” model} \\ 1/2, & \text{“-” model} \end{cases} \quad (3)$$

An evaluation of the second derivative of the conductivity with respect to the density of states, given later in this paper, yields completely different results for the “+” and “-” models:

$$\frac{\delta^2 \sigma}{\delta \tilde{\omega}^2} \propto |\tau|^\lambda, \quad \lambda = \begin{cases} -\varepsilon/18, & \text{“+” model} \\ +\varepsilon/2, & \text{“-” model} \end{cases} \quad (4)$$

A comparison of (2), (3), and (4) shows that the “+” model gives more abrupt functions and the “-” model less abrupt functions than self-consistent field theory, for which  $\varepsilon' = 7/2$ ,  $\beta = 1/2$ , and  $\lambda = 0$ . The diffusion coefficient is easily found from relations (1) and (4) as

$$D \propto |\tau|^{\beta+\lambda} \quad (5)$$

This result will be obtained in an independent manner. The results will be discussed in the Conclusion, and the most awkward mathematical part is relegated to Appendices A–C.

## 1. EVALUATION OF THE KINETIC COEFFICIENTS BY THE SELF-CONSISTENT-FIELD METHOD

### A. Nonideal excitonic insulator<sup>6</sup>

Let us assume that an ideal impurity-free system has the particle-hole symmetry

$$\xi_p = -\xi_{p+Q}, \quad (6)$$

where  $2Q$  is a reciprocal lattice vector and  $\xi_p$  is the energy reckoned from the Fermi level. Let us suppose that the interaction with impurities is of a short-range character and can be taken into account by perturbation theory. In this approximation the averaged function  $G_\omega(p)$  is of the form:

$$G_\omega^{-1}(p) = \begin{pmatrix} i\tilde{\omega} - \xi_p & \tilde{\Delta} \\ \tilde{\Delta} & i\tilde{\omega} + \xi_p \end{pmatrix}, \quad (7)$$

and the dependence of the quantities  $\tilde{\Delta}$  and  $\tilde{\omega}$  on the frequen-

cy  $\omega = (2n + 1)\pi T$  is given by the matching conditions:

$$i\tilde{\omega} = i\omega + \frac{i\tilde{\omega}}{2\tau[\tilde{\omega}^2 + \tilde{\Delta}^2]^{1/2}}, \quad \tilde{\Delta} = \Delta - \frac{\tilde{\Delta}}{2\tau[\tilde{\omega}^2 + \tilde{\Delta}^2]^{1/2}}, \quad (8)$$

where  $\tau$  is the relaxation time. Notation aside, the solution of Eq. (8) formally coincides with the corresponding solutions of the equations for a superconductor with a paramagnetic impurity.<sup>8</sup>

The “insulating gap” vanishes in accordance with a three-halves law:

$$\text{Gap} = [(\tau\Delta)^{3/2} - 1]^{2/3} \tau^{-1}, \quad \ln(\Delta/\Delta_0) = -\pi/4\tau\Delta. \quad (9)$$

Here  $\Delta$  is the value of the order parameter at  $T = 0$ , and  $\Delta_0$  is its value in the absence of impurities. The density of states vanishes by the square-root law

$$\nu = \nu_0 [1 - (\tau\Delta)^2]^{1/2}, \quad \nu_0 = \sum_p \delta(\xi_p), \quad (10)$$

where  $\nu_0$  is the density of states of the pure metal.

Using condition (6) and generalizing the derivation of the Kubo formula to the case of an anisotropic crystal, we obtain the following expressions for the electrical conductivity tensor ( $\omega_0$  is the external complex frequency):

$$Q_{ij} = -e^2 T \sum_{\omega, p} \text{Sp} \left\{ \tau^i \left[ G_\omega(p) \frac{\partial^2 \xi}{\partial p_i \partial p_j} + G_{\omega_+}(p) \tau^z G_{\omega_-}(p) \frac{\partial \xi}{\partial p_i} \frac{\partial \xi}{\partial p_j} \right] \right\},$$

where  $\omega_\pm = \omega \pm \omega_0/2$  and  $\tau^z$  is the Pauli matrix. Integrating the last sum over frequencies and then using definition (7), we reduce the expression for the electrical conductivity to the form

$$Q_{ij} = -e^2 T \sum_{\omega, p} \frac{\partial \xi}{\partial p_i} \frac{\partial \xi}{\partial p_j} \text{Sp} \{ G_{\omega_+}(p) \tau^z G_{\omega_-}(p) \tau^z - G_\omega(p) \tau^z G_\omega(p) \tau^z \}.$$

In the limit  $T = 0$  one can pass to an integration over the frequency and then expand in powers of  $\omega_0$ , obtaining

$$\sigma_{ij} = \frac{e^2}{2\pi} \sum_p \frac{\partial \xi}{\partial p_i} \frac{\partial \xi}{\partial p_j} \text{Sp} [G_+(p) \tau^z G_-(p) \tau^z], \quad (11)$$

$$G_\pm(p) = \lim_{\omega \rightarrow 0 \pm} G_\omega(p).$$

For a crystal of cubic symmetry  $\xi_p = \xi_{-p}$ , so that any impurity correction to the current vertex vanishes after integration over the variable  $p$ . For this reason the averaging of the product of the Green functions in (11) reduces to replacing them by the corresponding average values. The substitution of (7) into (11) and an elementary integration near the Fermi surface lead to the following:

$$\sigma = \sigma_0 [1 - (\tau\Delta)^2], \quad \sigma_0 = \frac{2}{3} \tau e^2 \sum_p \delta(\xi_p) (\partial \xi / \partial p)^2. \quad (12)$$

Here  $\sigma_0$  is the conductivity of the normal metal. Far from the transition point  $\sigma \approx \sigma_0$ . Close to the transition point the conductivity vanishes by a linear law,  $\sigma \approx 2\sigma_0(1 - \tau\Delta)$ .

The expression for the average value of the density-density correlator has an extremely awkward form even in the static limit. However, in the long-wavelength limit it is easily expressed in terms of the derivative of the Green function:

$$\Pi_0(0) = -iT \sum_{\mathbf{p}} \text{Sp} \frac{\partial G_{\omega}(\mathbf{p})}{\partial \omega},$$

as follows from the Ward identity. From this expression we find the inverse square of the screening radius for  $T = 0$ :

$$\kappa^2 = 4\pi e^2 v_0 [1 - (\tau\Delta)^2]^{1/2}. \quad (13)$$

Finally, using the Einstein relation (1), we obtain the diffusion coefficient

$$D = D_0 [1 - (\tau\Delta)^2]^{1/2}. \quad (14)$$

It should, of course, be kept in mind that the spatial dispersion of the dielectric constant and of the electrical conductivity begins at wavelengths of the order of the correlation length  $R_c$ :

$$R_c = \hbar v_0 / \Delta [1 - (\tau\Delta)^2]^{1/2}, \quad (15)$$

where  $v_0$  is the average velocity on the Fermi surface. Near the transition point, where  $\tau\Delta \sim 1$ , the correlation length exceeds the mean free path.

## B. Hubbard model and binary solid solution

The model of a binary solid solution with equal concentrations of the components and the Hubbard model with a half-filled band<sup>7</sup> have electron Green functions of the same form:

$$G_{\omega}(\mathbf{p}) = -i\tilde{\omega} (\varepsilon_0^2 + \omega^2 + i\tilde{\omega}\xi_{\mathbf{p}})^{-1}, \quad (16)$$

where  $\varepsilon_0$  is the spacing of the atomic levels in the solid solution or the energy of the electron-electron interaction in the Hubbard model. The function  $\tilde{\omega}$  satisfies a self-consistency condition of the type (8). For example, in the approximation of a large number of nearest neighbors<sup>2</sup>

$$i\tilde{\omega} = i\omega - g\varepsilon_0^2 \sum_{\mathbf{p}} \xi_{\mathbf{p}} (\varepsilon_0^2 + \omega^2 + i\tilde{\omega}\xi_{\mathbf{p}})^{-1}. \quad (17)$$

( $g = 1$  for the solid solution and  $g = 3$  for the Hubbard model).

In the coherent phase approximation (CPA) the self-consistency condition has a more complex form,<sup>7</sup> but all the basic properties near the  $M$ -transition point are determined by the character of the expansion of the self-consistency condition in powers of  $\tilde{\omega}$  and  $\omega$ . The expansion is of the usual Landau-Ginzburg form:

$$\tilde{\omega} = \omega + \tilde{\omega}\mu_2 - \tilde{\omega}^3\bar{\mu}_4/\varepsilon_0^2. \quad (18)$$

According to Hubbard,<sup>5</sup> in the CPA approximation one has

$$\mu_2 = g \sum_{\mathbf{p}} \xi_{\mathbf{p}}^2 \varepsilon_0^{-2}, \quad \mu_4 = g \sum_{\mathbf{p}} \xi_{\mathbf{p}}^4 \varepsilon_0^{-4},$$

$$\bar{\mu}_4 = \mu_4 - \mu_2^2/4.$$

Taking the usual formula (11) but without the anomalous Green functions and substituting Green function (16) in it, one can easily calculate the conductivity as

$$\sigma = \sigma_0 \sum_{\mathbf{p}} \frac{\tilde{\omega}^2(0)}{[\varepsilon_0^4 + \tilde{\omega}^2(0)\xi_{\mathbf{p}}^2]} \left( \frac{\partial \xi_{\mathbf{p}}}{\partial \mathbf{p}} \right)^2, \quad (19)$$

where  $\sigma_0 = e^2/3\pi\hbar a$  and  $a^3$  is the volume of the unit cell.

In the insulator phase  $\tilde{\omega}(0) = 0$ ; in the metal phase near the transition point we can use expansion (18). As a result, we obtain a linear law for the vanishing of the conductivity:

$$\sigma = \sigma_0 (\mu_2 - 1) \sum_{\mathbf{p}} (\partial \xi_{\mathbf{p}} / \partial \mathbf{p})^2 (\bar{\mu}_4)^{-1} \varepsilon_0^{-2}. \quad (20)$$

The diffusion coefficient can be calculated directly by averaging the retarded and advanced Green functions. Near the transition point

$$D = (a^2/3\hbar\varepsilon_0^2) \tilde{\omega}(0+) \sum_{\mathbf{p}} \left( \frac{\partial \xi_{\mathbf{p}}}{\partial \mathbf{p}} \right)^2. \quad (21)$$

The correlation length, the density of states, and the dielectric constant were evaluated in Refs. 2 and 8. Near the transition point

$$\tilde{R}_c^2 = \frac{g\hbar^2}{4\varepsilon_0^2} \sum_{\mathbf{p}} \left( \frac{\partial \xi_{\mathbf{p}}}{\partial \mathbf{p}} \right)^2 (\mu_2 - 1)^{-1}. \quad (22)$$

Comparison with (15) shows that for identical values of  $\tau = 1 - \mu_2 \sim [(\tau\Delta)^2 - 1]$  the self-consistent equation for an excitonic insulator has a wider domain of applicability than an equation of type (17). This is because at the  $M$ -transition point

$$\hbar^2 g \sum_{\mathbf{p}} \left( \frac{\partial \xi_{\mathbf{p}}}{\partial \mathbf{p}} \right)^2 \sim \varepsilon_0^2 a^2,$$

so that the ratio of the correlation lengths  $R_c/\tilde{R}_c$  is of the order of the mean free path measured in units of the interelectron distance. The physical reason for this difference is the absence of a Fermi surface in the Hubbard model, which leads to a strong intermixing of quasi-particles with different momenta and, in the final analysis, to their damping, which at low energies is of the same order as the energy. Formally returning to the analogy with the theory of phase transitions, we see that the Hubbard model is to the excitonic-insulator model as the Ising model is to the BCS model. The basic relationships in the region of strong correlations have a universal character.

## 2. THE DC CONDUCTIVITY IN THE REGION OF STRONG CORRELATIONS

### A. Renormalization-group equations

By analyzing the results of (20) and (12), it is easy to establish that in symmetric models the expansion of the conductivity tensor contains only even powers of the order parameter. In the first nonvanishing approximation the problem reduces to the evaluation of the trace of the product of four Green functions, as is shown in Fig. 1. Diagrams of the

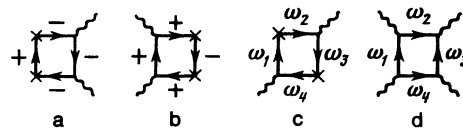


FIG. 1. Current vertices and the vertex  $\Gamma_3$  before averaging.

type in 1a and 1b are the average of the products of two Green functions, one of which is evaluated in the zeroth order and the other in the second order of perturbation theory in the parameter  $\tilde{\omega}$ . Diagrams of type 1c are averages of the products of two Green functions evaluated in the first order of perturbation theory. It follows from the general relation (11) that the lines joining the current vertices,  $G_+$  and  $G_-$ , represent Green functions with minimum frequencies of opposite signs. As we have already mentioned, impurity corrections to the current-type vertices need not be taken into account, since for cubic crystals they give zero upon integration over the electron momentum. There is also no need to take into account the impurity corrections to those corner vertices which are multiplied by the order parameter  $\tilde{\omega}$ , since they are already contained in the definition of  $\tilde{\omega}$ . For the sake of definiteness, let us first consider vertices of type 1c, in which current and scalar corner vertices alternate along the electron line. These vertices can be divided into two types: the first type includes those vertices which have one incoming and another outgoing electron line at every scalar vertex. The notation  $\tilde{\Gamma}_{\alpha\beta}^{(a)}(\omega_1, \omega_2, \omega_3, \omega_4)$  completely specifies the desired tetragonal vertex of the first type if the symbols  $\omega_1$  and  $\omega_3$  ( $\omega_2$  and  $\omega_4$ ) are taken to mean the frequencies of the electron lines coming into (going out of) the vector vertices. The definition implies the relation

$$\Gamma_{\alpha\beta}^{(a)}(\omega_1, \omega_2, \omega_3, \omega_4) = \Gamma_{\alpha\beta}^{(a)}(\omega_3, \omega_4, \omega_1, \omega_2).$$

The current vertex of the second type,  $\tilde{\Gamma}_{\alpha\beta}^{(b)}(\omega_1, \omega_2, \omega_3, \omega_4)$ , differs from  $\tilde{\Gamma}_{\alpha\beta}^{(a)}(\omega_1, \omega_2, \omega_3, \omega_4)$  in that  $\omega_2$  and  $\omega_3$  are the frequencies of the electron lines going out of the same scalar vertex;  $\omega_1$  and  $\omega_4$  are the frequencies of the electron lines coming into the other scalar vertex. In the zeroth approximation the vertex parts are independent and can be evaluated by perturbation theory. In the next approximation the corrections to  $\tilde{\Gamma}_{\alpha\beta}^{(a)}$  and  $\tilde{\Gamma}_{\alpha\beta}^{(b)}$  are expressed in terms of the scalar vertex part  $\Gamma_3(\omega_1, \omega_2, \omega_3, \omega_4)$ , which differs from  $\tilde{\Gamma}_{\alpha\beta}^{(b)}(\omega_1, \omega_2, \omega_3, \omega_4)$  in that the vector vertices  $\alpha$  and  $\beta$  are replaced by scalar vertices (see Figs. 1d and 2a,b). Each pair of parallel lines is averaged with the aid of a ladder summation. For a small total electron momentum  $s$  and for fixed frequencies of the electron lines in the same direction we obtain the correlator  $K_{\omega_1\omega_2}^{++}(s)$ . For a small momentum transfer  $q$  and for fixed frequencies of the electron lines with the opposite direction of the momentum we obtain the correlator  $K_{\omega_1\omega_2}^{+-}(q)$ . Elementary calculations (which are done in Appendix B for an excitonic insulator) show that at a small combined frequency  $\omega_1 = -\omega_2 \rightarrow 0$  the two correlators each have a pole of the diffusion type

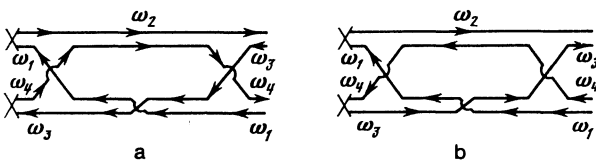


FIG. 2. Second-order perturbation theory for the current vertices  $\tilde{\Gamma}_{\alpha\beta}^{(a)}$  and  $\tilde{\Gamma}_{\alpha\beta}^{(b)}$ .

$$K_{-+}^{-1}(q) = K_{+-}^{-1}(q) \propto (\omega/\tilde{\omega} + R_1^2 q^2). \quad (23)$$

At small, equal frequencies  $\omega_1 = \omega_2 \rightarrow 0$  these correlators are singular only near the  $M$  transition [see Eq. (B.1)]:

$$K_{++}^{-1}(q) = K_{--}^{-1}(q) = (|\tau| + R_2^2 q^2). \quad (24)$$

Here  $|\tau|$  is the dimensionless distance from the transition point, and  $R_{1,2}$  are the diffusion and correlation lengths, which differ by  $|\tau|R$  near the transition point and for simplicity will henceforth be assumed equal to unity [see Eq. (B.3)]. In four-dimensional space the product of two correlators gives a logarithmic integration, so that after going over to the variable

$$t = \ln[q_m^2 / \max(q^2, s^2, |\tau|, \omega/\tilde{\omega})]$$

we obtain the following system of equations:

$$\begin{aligned} -\tilde{\Gamma}_{\alpha\beta}^{(a)}(1, 2, 3, 4) &= \tilde{\Gamma}_{\alpha\beta}^{(b)}(1, 2, 4, 3) \Gamma_3(2, 3, 1, 4) \\ -\tilde{\Gamma}_{\alpha\beta}^{(b)}(1, 2, 3, 4) &= \tilde{\Gamma}_{\alpha\beta}^{(a)}(1, 2, 4, 3) \Gamma_3(1, 3, 2, 4). \end{aligned} \quad (25)$$

Here and below  $\Gamma(1,2,3,4) \equiv \Gamma(\omega_1, \omega_2, \omega_3, \omega_4)$ , and the values of the logarithmic variable  $t$  are identical for all the functions appearing in Eq. (25).

Let us denote by  $\tilde{\Gamma}_{\alpha\beta}^{(a)}(\omega_1, \omega_2, \omega_3, \omega_4)$  and  $\tilde{\Gamma}_{\alpha\beta}^{(b)}(\omega_1, \omega_2, \omega_3, \omega_4)$  the two types of vertices for which the electron line of frequency  $\omega_1$  joins current corner vertices  $\alpha$  and  $\beta$ . The electron line with frequency  $\omega_2$  ( $\omega_4$ ) leaves (enters) the corner vertex  $\alpha$  ( $\beta$ ). These vertices differ by the direction of the electron line  $\omega_3$ . Equations are easily written for these vertices if one first writes out the diagrams containing every kind of product of two correlation functions (see Fig. 3):

$$\begin{aligned} &-\tilde{\Gamma}_{\alpha\beta}^{(a)}(1, 2, 3, 4) \\ &= \Gamma_{\alpha\beta}^{(b)}(1, 2, 2, 4) \Gamma_2(2, 2, 3, 4) + \Gamma_{\alpha\beta}^{(b)}(1, 2, 4, 4) \Gamma_2(4, 2, 3, 4) \\ &+ \Gamma_{\alpha\beta}^{(b)}(1, 2, 3, 4) \Gamma_3(2, 3, 4, 3) + \Gamma_{\alpha\beta}^{(b)}(1, 2, 1, 4) \Gamma_2(1, 2, 3, 4); \\ &-\tilde{\Gamma}_{\alpha\beta}^{(b)}(1, 2, 3, 4) \\ &= \Gamma_{\alpha\beta}^{(b)}(1, 2, 3, 4) \Gamma_4(2, 3, 4, 2) + \Gamma_{\alpha\beta}^{(b)}(1, 2, 4, 4) \Gamma_4(2, 3, 4, 4) \\ &+ \Gamma_{\alpha\beta}^{(a)}(1, 2, 3, 4) \Gamma_3(3, 2, 3, 4) + \Gamma_{\alpha\beta}^{(b)}(1, 2, 1, 4) \Gamma_4(2, 3, 4, 1). \end{aligned} \quad (26b)$$

Equation (26b) is found with the aid of Fig. 3 after reversing the direction of the line with frequency  $\omega_3$ .

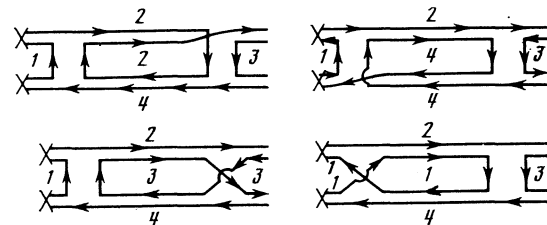


FIG. 3. Second-order perturbation theory for the current vertex  $\tilde{\Gamma}_{\alpha\beta}^{(b)}$ .

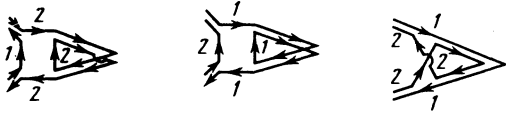


FIG. 4. First-order perturbation theory for the corner vertex  $\mathcal{F}^{(a),(1,2)}$ .

The equations for the scalar tetragonal vertices  $\Gamma_4$  have a somewhat more complex form. However, these equations do not contain the current vertices, and so their derivation and solution have been relegated to Appendices A, B, and C.

By applying the Ward identity to the inverse correlation functions, one can express the corrections to the diffusion coefficient and to the metallic order parameter in terms of the so-called corner vertices  $\mathcal{F}^{(a,c)}(\omega_1, \omega_2)$ . The vertex  $\mathcal{F}^{(c)}(\omega_1, \omega_2)$  is an irreducible set of diagrams (in the sense that they cannot be divided into two parts which are joined by two electron lines) having two incoming electron lines on one side and two outgoing electron lines on the other. The corner vertex  $\mathcal{F}^{(a)}(\omega_1, \omega_2)$  differs from  $\mathcal{F}^{(c)}(\omega_1, \omega_2)$  in that the direction of the second electron line is reversed.

We obtain the equations for  $\mathcal{F}^{(a)}(\omega_1, \omega_2)$  with the aid of first-order perturbation theory (see Fig. 4):

$$\begin{aligned}
 & -\dot{\mathcal{F}}^{(a)}(1, 2) \\
 & = \Gamma_2(2, 2, 1, 2) \mathcal{F}^{(c)}(2, 2) + \Gamma_2(1, 1, 2, 1) \mathcal{F}^{(c)}(1, 1) \\
 & \quad + \Gamma_3(1, 2, 1, 2) \mathcal{F}^{(e)}(1, 2); \\
 & -\dot{\mathcal{F}}^{(e)}(1, 2) \\
 & = \Gamma_4(1, 2, 2, 2) \mathcal{F}^{(c)}(2, 2) + \Gamma_4(2, 1, 1, 1) \mathcal{F}^{(c)}(1, 1) \\
 & \quad + \Gamma_3(1, 2, 1, 2) \mathcal{F}^{(a)}(1, 2).
 \end{aligned} \tag{27}$$

It follows from the definition that the vertex parts  $\mathcal{F}^{(a)}$  and  $\mathcal{F}^{(c)}$  are symmetric functions of their arguments. The common coefficient on the right-hand sides of Eqs. (22)–(24) is assumed equal to unity; this means that all the scalar tetragonal vertices  $\Gamma_k$  have been rendered dimensionless by the same positive constant.

## B. Evaluation of the critical exponent $\lambda$

A study (given in Appendix C) of the equation for  $\Gamma_k$  shows that two types of solutions exist. One of these, the most symmetric, is the “+” model, in which all the  $\Gamma_k$  are identical. The other solution, the “-” model, corresponds to the solution  $\Gamma_1 = \Gamma_2 = -\Gamma_3 = \Gamma_4$ , which is less symmetric but more stable,<sup>3</sup> since in the case of identical, small frequency arguments it asymptotically approaches a stable center. In both cases the vertices  $\Gamma_k$  are expressed in terms of vertex  $\Gamma_1$  and share with it a cyclic invariance with respect to the frequency arguments.

Let us consider the solutions of Eqs. (25)–(27) for the case  $\omega_k \rightarrow 0^\pm$ , which corresponds to the static values of the kinetic coefficients in the limit as  $T \rightarrow 0$ .

It is convenient to introduce the following notation:

$$\Gamma_1 = \Gamma_2 = \pm \Gamma_3 = \Gamma_4 = \Gamma,$$

$$A = \Gamma(0+, 0+, 0+, 0+) = \Gamma(0-, 0-, 0-, 0-),$$

$$B = \Gamma(0+, 0-, 0-, 0-) = \Gamma(0-, 0+, 0+, 0+) = \dots,$$

$$C = \Gamma(0+, 0+, 0-, 0-) = \dots, \tag{28}$$

$$D = \Gamma(0+, 0-, 0+, 0-) = \dots$$

The ellipses stand for equations obtained by cyclic permutation of the arguments. For fixed  $\Gamma$  the equations for the current and corner vertices separate into four pairs of independent linear differential equations. All the antisymmetric combinations made up of each pair are expressed in terms of one another and will be assumed equal to zero; forgoing of this assumption does not give qualitatively new results. With these considerations in mind, let us define four unknown functions:

$$\Gamma_{\alpha\beta} = \frac{1}{2} [\Gamma_{\alpha\beta}^{(a)}(+, -, -, +) + \Gamma_{\alpha\beta}^{(b)}(+, -, +, -)], \tag{29}$$

$$\Gamma_{\alpha\beta} = \Gamma_{\alpha\beta}^{(a)}(+, -, -, -) = \Gamma_{\alpha\beta}^{(b)}(+, -, -, -),$$

$$\mathcal{F} = \mathcal{F}^{(a)}(+, +) = \mathcal{F}^{(e)}(+, +) = \mathcal{F}^{(a)}(-, -) = \mathcal{F}^{(c)}(-, -),$$

$$\tilde{\mathcal{F}} = \mathcal{F}^{(a)}(+, -) = \mathcal{F}^{(c)}(+, -).$$

Equations (25)–(27) are thereby transformed to the following:

$$\begin{aligned}
 -\dot{\Gamma}_{\alpha\beta} & = \pm C \Gamma_{\alpha\beta}, \quad -\dot{\tilde{\Gamma}}_{\alpha\beta} = (2 \pm 1) A \Gamma_{\alpha\beta} + B \tilde{\Gamma}_{\alpha\beta}; \\
 -\dot{\mathcal{F}} & = (2 \pm 1) A \mathcal{F}, \quad -\dot{\tilde{\mathcal{F}}} = 2B \mathcal{F} \pm D \tilde{\mathcal{F}}.
 \end{aligned} \tag{30}$$

The  $\pm$  signs correspond to the “ $\pm$ ” models. The corner vertex parts are derivatives of the inverse correlation functions. For this reason the vertex part  $\mathcal{F}$  governs the corrections to the metallic order parameter  $\tilde{\omega}^3$ , while the corner vertex part  $\tilde{\mathcal{F}}$  determines the diffusion coefficient

$$D \propto \tilde{\omega} / \tilde{\mathcal{F}}. \tag{31}$$

Comparison with perturbation theory shows that the second derivative of the conductivity with respect to the order parameter  $\tilde{\omega}$  is given by a linear combination of current vertices

$$\delta^2 \sigma / \delta \tilde{\omega}^2 = \Gamma_{\alpha\beta}^{(e)} = \Gamma_{\alpha\beta} - 2 \Gamma_{\alpha\beta}. \tag{32}$$

It is shown in Appendices B and C that two types of solutions correspond in the “+” model to fixed singular points whose coordinates can be reconciled with perturbation theory, namely

$$A = B = -C = D, \quad A = A_0 (1 + 9A_0 t)^{-1} \tag{33'}$$

and

$$B = \frac{81}{88} A, \quad C = -\frac{9\sqrt{15}}{44} A, \quad D = \frac{18}{11} A. \tag{33''}$$

In the “-” model there is just one singular point, which corresponds to solution (33'), but with  $A = A_0 (1 + A_0 t)^{-1}$ . The quantity  $A_0$  is positive and hereafter will, for simplicity, be assumed equal to unity. Let us write out the solutions of Eqs. (30) for the “+” model:

$$\begin{aligned}
 \Gamma_{\alpha\beta} & = \Gamma_{\alpha\beta}(0) A^{c/9}, \quad \mathcal{F} = \mathcal{F}(0) A^{1/4}, \\
 \Gamma_{\alpha\beta} & = \Gamma_{\alpha\beta}(0) A^{1/4} - \frac{b \Gamma_{\alpha\beta}(0)}{3-c} (A^{c/9} - A^{1/4}),
 \end{aligned} \tag{34}$$

$$\tilde{\mathcal{F}} = \tilde{\mathcal{F}}(0) A^{d/9} + \frac{2b}{3-d} \mathcal{F}(0) (A^{1/3} - A^{d/9}).$$

Here  $c = C/A$ ,  $b = B/A$ , and  $d = D/A$ . In the space of  $4 - \varepsilon$  dimensions and close to the transition point the variable  $t$  should be replaced by  $|\tau|^{-\varepsilon/2}$ , so that as  $|\tau| \rightarrow 0$

$$\Gamma_{\alpha\beta}^{(a)} \propto A^{c/9} \propto |\tau|^{ec/18}, \quad \tilde{\mathcal{F}} \propto A^{d/9} \propto |\tau|^{ed/18}. \quad (35)$$

It is easy to see that the final results (35) can be reconciled with the Einstein relation (1) if the solution is Eq. (33') with  $b = -c = d = 1$ . Using the results of Ref. 3, according to which  $\beta = 1/2 - \varepsilon/6$ , we obtain with the aid of (31) and (32):

$$\begin{aligned} \tilde{\omega} \propto \nu \propto \kappa^2 \propto |\tau|^\beta = |\tau|^{1/2 - \varepsilon/6}, \\ \sigma \sim \tilde{\omega}^2 |\tau|^{-\varepsilon/18} \sim |\tau|^{1-7\varepsilon/18}, \quad D \sim \tilde{\omega} |\tau|^{-\varepsilon/18} \sim |\tau|^{1/2 - 2\varepsilon/9}. \end{aligned} \quad (36)$$

In precisely the same way we determine the critical exponents in the “-” model:

$$\Gamma_{\alpha\beta} = \Gamma_{\alpha\beta}(0) A;$$

$$\tilde{\mathcal{F}} = (\tilde{\mathcal{F}}(0) - \mathcal{F}(0)) A^{-1} + \mathcal{F}(0) A, \quad \mathcal{F} = \mathcal{F}(0) A, \quad (37)$$

$$\Gamma_{\alpha\beta} = \Gamma_{\alpha\beta}(0) A + \Gamma_{\alpha\beta}(0) A \ln A.$$

Allowance for a dependence of the  $\ln A$  type obviously exceeds the accuracy of the parquet approximation used here. For this reason the last term in (37) should be discarded. With this remark in mind, we find the critical exponents (according to Ref. 3, in the “-” model  $\beta = 1/2$ )

$$\tilde{\omega} \sim \nu \sim \kappa^2 \sim |\tau|^{1/2}, \quad \sigma \sim |\tau|^{1+\varepsilon/2}, \quad D \sim |\tau|^{1/2 + \varepsilon/2}. \quad (38)$$

This last result obviously satisfies the Einstein relation, and formulas (36) and (38) solve the problem posed in this paper.

### 3. CONCLUSION

We have thus seen that one can make the rather important qualitative assertion that it is in the region of “minimum” conductivity that correlation effects are important. In this region as  $\varepsilon \rightarrow 1$  the “-” model, in terms of its critical exponents, approaches percolation theory,<sup>9</sup> for which  $\sigma \sim |\tau|^{8/5}$ ; the more abrupt “+” model gives results which are close to the experimental data for disordered semiconductors,<sup>10,11</sup> for which  $\sigma \approx |\tau|^{1/2}$ . In the region of applicability of the self-consistent-field method we have  $\sigma \sim |\tau|$ , and our results coincide with one of the limiting cases of the modern theory of localization.<sup>12</sup>

As for the experiments near the  $M$ -transition point, the determination of the critical exponents is masked by fluctuations deriving from the structural instability accompanying the transition to the insulating state.

A well-known exception to this rule is the phase transition in the isovalent solid solution  $\text{Ni}(\text{Se}_x\text{S}_{1-x})_2$  (Ref. 13) and, in particular, in  $\text{NiS}_2$  (Ref. 14). The electronic structure of this compound is such that at any  $x$  the conduction band is exactly half filled. At the transition point there is an extremely slight change in the volume of the pyrite-type unit

cell<sup>15</sup> (without a change in shape). This change for  $T = 0$  is accompanied by a change in the resistivity by not less than three orders of magnitude.<sup>16</sup> As a result, the conductivity turns out to be of the order of  $10 (\Omega\text{-cm})^{-1}$ —significantly below its “minimum” value. The question of which of the models—the percolation, “+”, or “-” model—describes this transition should be settled by low-temperature experimental measurements of the critical exponents.

The author is indebted to M. I. Dushenat for assistance in the numerical calculations.

## APPENDIX A

### Equations for the scalar vertices

The vertex parts  $\Gamma_k$  for arbitrary frequencies are defined in absolute correspondence with their description for all positive  $\omega$ .<sup>3</sup> The vertex parts  $\Gamma_1$  are the same as the current vertices  $\tilde{\Gamma}_{\alpha\beta}^{(a)}$ , but with the density operators replaced by unity. Here the vertex  $\Gamma_1(\omega_1, \omega_2, \omega_3, \omega_4)$  is invariant with respect to cyclic permutations of its arguments. For a fixed direction of going around along the electron lines, the direction of the momentum of the electron line with frequency  $\omega_1$  at the vertices  $\Gamma_2(\omega_1, \omega_2, \omega_3, \omega_4)$  is opposite to the direction of the momentum of all the other lines. The vertex part  $\Gamma_3(\omega_1, \omega_2, \omega_3, \omega_4)$  differs from  $\Gamma_1$  by the interchange of the directions of the electron lines with the third and fourth frequency arguments. The vertex part  $\Gamma_4(\omega_1, \omega_2, \omega_3, \omega_4)$  differs from  $\Gamma_1$  in a similar way, but for the lines of the second and fourth arguments. Here  $\Gamma_4$  is invariant with respect to a double cyclic permutation.

For every given type of diagram there is a definite sequential arrangement of the momenta of the electron lines. Therefore, to write down the equations it is sufficient to sketch the various types of second-order diagrams with the electron lines in the direction corresponding to the given type of diagram, and then do a cyclic permutation of the indices of the  $\omega_k$ . For example, for a vertex of the first type,  $\Gamma_1(\omega_1, \omega_2, \omega_3, \omega_4)$ , we have the 3 types of diagrams shown in Fig. 5. In diagrams 5a, b it is necessary to do a four-fold cyclic permutation (CP) of  $\omega_1, \omega_2, \omega_3$ , and  $\omega_4$ . One is readily convinced that in diagram 5c this permutation leads to a topologically equivalent diagram of the same form. After transforming to the logarithmic variable we obtain the following:

$$\begin{aligned} & -\Gamma_1(1, 2, 3, 4) \\ & = \{[\Gamma_2(4, 4, 1, 2) \Gamma_2(4, 2, 3, 4) + \Gamma_2(3, 4, 1, 2) + \Gamma_3(2, 3, 4, 3)] \\ & \quad + [\text{CP}]\} + \Gamma_3(1, 2, 4, 3) \Gamma_3(2, 3, 1, 4). \end{aligned} \quad (\text{A.1})$$

Here and below  $\Gamma_k(1, 2, 3, 4) \equiv \Gamma_k(\omega_1, \omega_2, \omega_3, \omega_4)$ . We obtain the remaining four equations by changing the direction of one or two of the electron lines. Here, however, it is necessary to sketch and then write out each of the nine diagrams of second-order perturbation theory:

$$\begin{aligned} & -\dot{\Gamma}_2(1, 2, 3, 4) \\ & = \Gamma_2(1, 1, 3, 4) \Gamma_2(1, 2, 3, 1) + \Gamma_2(2, 2, 3, 4) \Gamma_4(1, 4, 2, 2) \end{aligned}$$

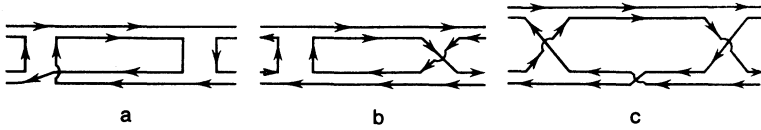


FIG. 5. Skeleton diagrams of second-order perturbation theory for the scalar vertex  $\Gamma_1$ .

$$\begin{aligned}
 & +\Gamma_2(4, 2, 3, 4)\Gamma_4(4, 1, 2, 4) + \Gamma_3(2, 3, 3, 1)\Gamma_3(3, 4, 1, 3) \\
 & +\Gamma_2(2, 1, 2, 3)\Gamma_3(3, 4, 1, 2) + \Gamma_2(4, 3, 4, 1)\Gamma_3(1, 4, 3, 2) \\
 & +\Gamma_1(1, 2, 3, 4)\Gamma_3(1, 4, 1, 2) + \Gamma_3(2, 3, 4, 3)\Gamma_4(1, 4, 3, 2) \\
 & \quad + \Gamma_2(2, 1, 3, 4)\Gamma_2(4, 2, 3, 1); \quad (\text{A.2})
 \end{aligned}$$

$$\begin{aligned}
 & -\Gamma_3(1, 2, 3, 4) \\
 & = \{[\Gamma_3(1, 2, 2, 4)\Gamma_2(2, 2, 4, 3) + \Gamma_3(1, 2, 3, 1)\Gamma_2(1, 4, 3, 1) \\
 & + \Gamma_2(1, 4, 3, 2)\Gamma_2(2, 1, 2, 3) + \Gamma_2(2, 1, 4, 3)\Gamma_2(1, 4, 1, 2)] \\
 & + [(1, 2, 3, 4) \rightarrow (4, 3, 2, 1)]\} + \Gamma_3(1, 3, 2, 4)\Gamma_1(1, 2, 4, 3); \quad (\text{A.3})
 \end{aligned}$$

$$\Gamma_3(1, 2, 3, 4) = \Gamma_3(4, 3, 2, 1), \quad (\text{A.3}')$$

$$\begin{aligned}
 & -\Gamma_4(1, 2, 3, 4) \\
 & = \{[\Gamma_4(1, 2, 4, 4)\Gamma_4(3, 4, 4, 2) + \Gamma_2(1, 4, 3, 2)\Gamma_3(3, 4, 3, 2)] \\
 & + [(1, 2, 3, 4) \rightarrow (2, 1, 3, 4)] + [(1, 2, 3, 4) \rightarrow (4, 3, 2, 1)] \\
 & + [(1, 2, 3, 4) \rightarrow (3, 4, 1, 2)]\} + \Gamma_4(1, 2, 4, 3)\Gamma_4(1, 3, 2, 4); \quad (\text{A.4})
 \end{aligned}$$

$$\Gamma_4(1, 2, 3, 4) = \Gamma_4(2, 1, 4, 3) = \Gamma_4(4, 3, 2, 1) = \Gamma_4(3, 4, 1, 2). \quad (\text{A.4}')$$

The two additional symmetry relations (A.3') and (A.4') can be obtained by changing the direction of going around along the electron lines.

Using all the relations and the cyclic invariance of the vertex  $\Gamma_1$ , one can conclude that Eqs. (A.1)–(A.4) admit the solutions  $\Gamma_1 = \Gamma_2 = \Gamma_3 = \Gamma_4$ , i.e., the “+” model, and  $\Gamma_1 = \Gamma_2 = -\Gamma_3 = \Gamma_4$ , i.e., the “-” model. These models are examined separately below for the case of extremely low frequencies.

## APPENDIX B

### Initial conditions for the “+” model

In this model all the results are independent of the direction of the electron momenta. The eight-point vertices depend on both the total momentum  $\mathbf{s}$  and on the momentum transfer  $\mathbf{q}$ . In perturbation theory their analytical expression is determined by the three diagrams shown in Fig. 6. The wavy lines represent the ladder sums:  $K_c$  for frequencies of the same sign and  $K_g$  for frequencies of opposite sign. In the theory of a nonideal excitonic insulator one associates with each closed tetragon (or triangle) the trace of the four (or three) electron Green functions, and this trace must then be integrated over the internal electron momentum.

Using the explicit expression for the Green function of an excitonic insulator (7), we obtain for all frequencies of the

same sign

$$\sum_{\mathbf{p}} \text{Sp } G_{\omega^+}(p) = \frac{\pi v_0 \Delta^2 (\Delta^2 - 4\tilde{\omega}^2)}{(\tilde{\omega}^2 + \Delta^2)^{3/2}},$$

$$\sum_{\mathbf{p}} \text{Sp } G_{\omega^-}(p) = -\frac{3i\tilde{\omega}\pi v_0 \Delta^2}{(\tilde{\omega}^2 + \Delta^2)^{3/2}} \quad (\text{B.1})$$

$$K_c^{-1}(\mathbf{Q}) = 4\pi v_0 \tau \left[ 1 - \frac{\Delta^2}{2\tau(\tilde{\omega}^2 + \Delta^2)^{1/2}} + R_1^2 Q^2 \right],$$

where

$$R_1^2 = \frac{v_{hk} \Delta^2}{8\tau v_0 d (\tilde{\omega}^2 + \Delta^2)^{3/2}},$$

$$v_{hk} = \sum_{\mathbf{p}} \delta(\xi_{\mathbf{p}}) \left( \frac{\partial \xi}{\partial \mathbf{p}} \right)^2, \quad v_0 = \sum_{\mathbf{p}} \delta(\xi_{\mathbf{p}}).$$

Using these formulas, let us write an expression for the vertex part of all  $\omega \rightarrow 0^+$ :

$$\begin{aligned}
 & A(\mathbf{s}, \mathbf{q}) \\
 & = \frac{\pi v_0 \Delta^2}{(\tilde{\omega}^2 + \Delta^2)^{3/2}} \left\{ 4\tilde{\omega}^2 - \Delta^2 + \frac{9\pi v_0 \tilde{\omega}^2 \Delta^2}{(\tilde{\omega}^2 + \Delta^2)^{3/2}} [K_c(\mathbf{s}) + K_c(\mathbf{q})] \right\}. \quad (\text{B.2})
 \end{aligned}$$

Correlators of the diffusion type are made up of ladder diagrams with two electron lines whose frequencies are of opposite sign:

$$\begin{aligned}
 & K_g^{-1}(\mathbf{Q}) = 4\pi v_0 \tau \left\{ 1 - \frac{1}{2\tau(\tilde{\omega}^2 + \Delta^2)^{1/2}} + R_2^2 Q^2 \right\}, \\
 & R_2^2 = \frac{v_{hk}}{8\tau v_0 d (\tilde{\omega}^2 + \Delta^2)^{3/2}}. \quad (\text{B.3})
 \end{aligned}$$

The vertex parts of the  $B$  type have three frequencies of the same sign and one frequency of the opposite sign. One must therefore evaluate the following two quantities:

$$\sum_{\mathbf{p}} \text{Sp } G_{\omega^+}(\mathbf{p}) G_{-\omega}(\mathbf{p}) = \frac{\pi v_0 (2\Delta^2 - \tilde{\omega}^2)}{2(\tilde{\omega}^2 + \Delta^2)^{3/2}},$$

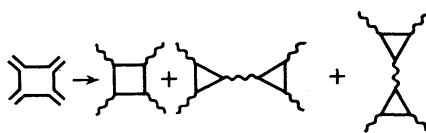


FIG. 6. Averaging of scalar vertices in zeroth order of perturbation theory.

$$\sum_{\mathbf{p}} \text{Sp} G_{\omega^2}(\mathbf{p}) G_{-\omega}(\mathbf{p}) = -\text{Sp} \sum_{\mathbf{p}} G_{-\omega^2}(\mathbf{p}) G_{\omega}(\mathbf{p}) \quad (\text{B.4})$$

$$= -\frac{i\pi\nu_0\tilde{\omega}}{(\tilde{\omega}^2 + \tilde{\Delta}^2)^{3/2}}.$$

Using (B.3) and (B.4), we find the vertex part of the  $B$  type for the particular case  $-\omega_1 = \omega_2 = \omega_3 = \omega_4 = \omega$ :

$$B_{\omega}(\mathbf{s}, \mathbf{q}) = \frac{\pi\nu_0}{(\tilde{\omega}^2 + \tilde{\Delta}^2)^{3/2}} \left\{ \frac{\tilde{\omega}^2 - 2\tilde{\Delta}^2}{2} + \frac{\pi\nu_0\tilde{\omega}^2}{(\tilde{\omega}^2 + \tilde{\Delta}^2)^{3/2}} \right. \\ \left. \times \left[ \frac{3\tilde{\Delta}^2}{\tilde{\omega}^2 + \tilde{\Delta}^2} K_c(\mathbf{s}) + K_g(\mathbf{q}) \right] \right\}. \quad (\text{B.5})$$

For zero total momentum

$$K_c(0) = (\tilde{\omega}^2 + \tilde{\Delta}^2)^{3/2} / 2\pi\nu_0\tilde{\omega}^2,$$

so that in this limit

$$B_{\omega}(0, \mathbf{q}) = \frac{\pi\nu_0}{(\tilde{\omega}^2 + \tilde{\Delta}^2)^{3/2}} \left\{ \frac{1}{2} + \frac{\pi\nu_0\tilde{\omega}^2}{(\tilde{\omega}^2 + \tilde{\Delta}^2)^{3/2}} K_g(\mathbf{q}) \right\} > 0. \quad (\text{B.6})$$

The vertex part  $A_{\omega}(\mathbf{s}, \mathbf{q})$  has an analogous feature; for this part

$$A_{\omega}(0, \mathbf{q}) = A_{\omega}(\mathbf{q}, 0) \\ = \frac{\pi\nu_0\tilde{\Delta}^2}{(\tilde{\omega}^2 + \tilde{\Delta}^2)^{3/2}} \left\{ \frac{7\tilde{\Delta}^2 + 8\tilde{\omega}^2}{2} + \frac{9\pi\nu_0\tilde{\omega}^2\tilde{\Delta}^2}{(\tilde{\omega}^2 + \tilde{\Delta}^2)^{3/2}} K_c(\mathbf{q}) \right\}, \quad (\text{B.7})$$

$$A_{\omega}(0, 0) = \frac{4\pi\nu_0\tilde{\Delta}^2(2\tilde{\Delta}^2 + \tilde{\omega}^2)}{(\tilde{\omega}^2 + \tilde{\Delta}^2)^{3/2}}.$$

In the opposite limiting case,  $R^2 Q^2 \rightarrow \infty$ , and also in the insulating phase, where  $\tilde{\omega}(0) = 0$ , the two vertex parts are equal and negative. The  $C$  and  $D$  vertices are evaluated in a completely analogous way. First we find

$$\sum_{\mathbf{p}} \text{Sp} G_{\omega^2}(\mathbf{p}) G_{-\omega^2}(\mathbf{p}) = \sum_{\mathbf{p}} \text{Sp} (G_{\omega}(\mathbf{p}) G_{-\omega}(\mathbf{p}))^2 \\ = \frac{\pi\nu_0}{(\tilde{\omega}^2 + \tilde{\Delta}^2)^{3/2}}, \quad (\text{B.8})$$

and then, with the aid of (B.4) and Fig. 1, we determine the dependence on the total momentum and momentum transfer:

$$C_{\omega}(\mathbf{s}, \mathbf{q}) = -\frac{\pi\nu_0}{(\tilde{\omega}^2 + \tilde{\Delta}^2)^{3/2}} \left\{ 1 + \frac{\pi\nu_0\tilde{\omega}^2}{(\tilde{\omega}^2 + \tilde{\Delta}^2)^{3/2}} [K_g(\mathbf{s}) + K_g(\mathbf{q})] \right\}, \quad (\text{B.9})$$

$$D_{\omega}(\mathbf{s}, \mathbf{q}) = -\frac{\pi\nu_0}{(\tilde{\omega}^2 + \tilde{\Delta}^2)^{3/2}} \left\{ 1 - \frac{\pi\nu_0\tilde{\omega}^2}{(\tilde{\omega}^2 + \tilde{\Delta}^2)^{3/2}} [K_c(\mathbf{s}) + K_c(\mathbf{q})] \right\}. \quad (\text{B.10})$$

It follows from these formulas that vertex  $C$  is always negative, while vertex  $D$  is negative and vanishes as  $\mathbf{s}, \mathbf{q} \rightarrow 0$ . For the far metallic region this property of the vertex  $D$  was discovered in Ref. 17. In the Hubbard model and the model of a binary solid solution the scalar vertices have the following properties which will be important later:  $C < 0$  everywhere,  $A > 0$  and  $B > 0$  in the metallic phase.

## APPENDIX C

### 1. Stability of the “+” model

After passing to the limit  $\omega_k \rightarrow 0 \pm$  we introduce the notation (28) in equations (A.1)–(A.4). As a result, we obtain the following system of equations:

$$-A = 9A^2, \quad -\dot{B} = 3AB + 4B^2 + C^2 + DB, \quad (\text{C.1}) \\ -\dot{C} = 8BC + DC, \quad -\dot{D} = 4B^2 + C^2 + 4D^2.$$

This system admits the solution  $C \equiv 0$ , so that the  $C = 0$  plane is the separatrix. The initial conditions give  $C < 0$ , so that all the physical solutions are found in the region of negative  $C$ , while the singular points lying on the  $C = 0$  plane and in the region  $C > 0$  are inaccessible under the initial conditions (B.10). For studying system (C.1) in the region  $C < 0$ , it is convenient to change to the variables

$$x = -A/C, \quad y = -B/C, \quad z = -D/C, \\ \psi = -1/C, \quad ds = -Cdt, \quad dt = \psi ds, \quad (\text{C.2})$$

in which

$$\partial x / \partial s = x(8y + z) - 9x^2, \quad \partial y / \partial s = 4y^2 - 3xy - 1, \quad (\text{C.3}) \\ \partial z / \partial s = 8yz - 4y^2 - 3z^2 - 1, \quad \partial \psi / \partial s = \psi(8y + z).$$

In the new variables the plane  $x = 0$  is the separatrix, and it can be shown that on this plane there are no real singular points. For  $x \neq 0$  there are four singular points:

$$P_1^{(\pm)} = \pm(1, 1, 1), \quad P_2^{(\pm)} = \pm(44/9\sqrt{15}, 9/2\sqrt{15}, 8/\sqrt{15}). \quad (\text{C.4})$$

According to (B.6), in the metallic phase and at small total momentum and momentum transfer, the vertex part  $A > 0$ . The opposite inequality holds throughout the entire existence region of the insulating phase. Therefore, the region of interest to us,  $x > 0$ , can be called the metallic region. In this region there are only two singular points,  $P_1^{(+)}$  and  $P_2^{(+)}$ . The point  $P_1^{(+)}$  is a saddle point in the  $xy$  plane at  $z = 1$  ( $\lambda_+^{(1)} = 3, \lambda_-^{(1)} = -7$ ); the direction parallel to the  $z$  axis is the proper direction ( $\lambda_z^{(1)} = +2$ ); the characteristic equation corresponding to the point  $P_2^{(+)}$  is of the form  $\lambda^3 + 8.977\lambda^2 - 9.103\lambda - 53.068 = 0$ , from which we find

$$\lambda_1^{(2)} = 2.573, \quad \lambda_2^{(2)} = -2.207, \quad \lambda_3^{(2)} = -9.343. \quad (\text{C.5})$$

### 2. Stability of “-” model

Let us set  $\Gamma_1 = \Gamma_2 = -\Gamma_3 = \Gamma_4$  in Eqs. (A.1)–(A.4), and then pass to the limit  $\omega_k \rightarrow 0 \pm$ . Using the same notation as before (28), we obtain the equations for the “-” model:

$$-A = A^2, \quad -\dot{B} = AB + C^2 - BD, \quad (\text{C.6}) \\ -\dot{C} = CD, \quad -\dot{D} = C^2 + 4B^2 - 4D^2.$$

The  $C = 0$  plane is the separatrix, and therefore for  $C < 0$  we again change to the variables given in (C.2):

$$\partial x / \partial s = xz - x^2, \quad \partial y / \partial s = 2yz - 1 - xy, \quad (\text{C.7}) \\ \partial z / \partial s = 5z^2 - 4y^2 - 1, \quad \partial \psi / \partial s = \psi z.$$

On the separatrix plane  $x = 0$  we find two unstable centers:

$$Q_2^{(\pm)} = \left( 0, \left( \frac{\sqrt{21}-1}{8} \right)^{1/2}, \left( \frac{\sqrt{21}+1}{10} \right)^{1/2} \right). \quad (\text{C.8})$$

In the region of interest, the metallic region  $x > 0$ , there is just one saddle-type singular point  $Q_1 = (1, 1, 1)$  with two positive and one negative eigenvalues:

$$\lambda_1^{(1)} = 3, \quad \lambda_{2,3}^{(1)} = (7 \pm \sqrt{73})/2. \quad (\text{C.9})$$

The third point  $Q_3 = (-1, -1, -1)$  has the same eigenvalues but is found in the insulator-phase region ( $x < 0$ ).

<sup>1</sup>F. J. Wegner, Z. Phys. B **35**, 207 (1979).

<sup>2</sup>R. O. Zaitsev, Zh. Eksp. Teor. Fiz. **75**, 2362 (1978) [Sov. Phys. JETP **48**, 1198 (1978)].

<sup>3</sup>R. O. Zaitsev, Zh. Eksp. Teor. Fiz. **84**, 652 (1983) [Sov. Phys. JETP **57**, 377 (1983)].

<sup>4</sup>N. F. Mott, Phys. Rev. Lett. **31**, 466 (1973).

<sup>5</sup>J. Hubbard, Proc. R. Soc. London Ser. A **281**, 401 (1964).

<sup>6</sup>J. Zittartz, Phys. Rev. **164**, 575 (1967).

<sup>7</sup>B. Velický, S. Kirkpatrick, and H. Ehrenreich, Phys. Rev. **175**, 747 (1968).

<sup>8</sup>R. O. Zaitsev, Zh. Eksp. Teor. Fiz. **78**, 1132 (1980) [Sov. Phys. JETP **51**, 571 (1980)].

<sup>9</sup>S. Kirkpatrick, Phys. Rev. Lett. **27**, 1722 (1971).

<sup>10</sup>T. F. Rosenbaum, K. Anders, G. A. Thomas, and R. N. Bhatt, Phys. Rev. Lett. **45**, 1723 (1980).

<sup>11</sup>B. W. Dodson, W. L. McMillan, J. M. Mochel, and R. C. Dynes, Phys. Rev. Lett. **46**, 46 (1981).

<sup>12</sup>F. J. Wegner, Z. Phys. B **25**, 327 (1976).

<sup>13</sup>F. Gauter, G. Krill, M. F. Lapiere, P. Panissod, C. Robert, G. Czjzek, J. Fink, and H. Schmidt, Phys. Lett. A **53**, 31 (1975).

<sup>14</sup>N. Mori, T. Mitsui, and S. Yomo, Solid State Commun. **13**, 1083 (1973).

<sup>15</sup>S. Endo, T. Mitsui, and T. Miyadai, Phys. Lett. A **46**, 29 (1973).

<sup>16</sup>H. S. Jarrett, R. J. Bouchard, J. L. Gillson, G. A. Jones, S. M. Marcus, and J. F. Weiher, Mater. Res. Bull. **8**, 877 (1973).

<sup>17</sup>L. P. Gor'kov, A. I. Larkin, and D. E. Khmel'nitskiĭ, Pis'ma Zh. Eksp. Teor. Fiz. **30**, 248 (1979) [JETP Lett. **30**, 228 (1979)].

Translated by Steve Torstveit